1 **SARS-CoV-2 variants B.1.351 and B.1.1.248: Escape from therapeutic**

2 **antibodies and antibodies induced by infection and vaccination**

3

4 Markus Hoffmann[1,2,10,*], Prerna Arora[1,2,10], Rüdiger Groß[3,10], Alina Seidel[3,10], Bojan Hörnich[4],

5 Alexander Hahn[4], Nadine Krüger[1], Luise Graichen[1], Heike Hofmann-Winkler[1],

6 Amy Kempf[1,2], Martin Sebastian Winkler[5], Sebastian Schulz[6], Hans-Martin Jäck[6], Bernd

7 Jahrsdörfer[7], Hubert Schrezenmeier[7], Martin Müller[8], Alexander Kleger[8], Jan Münch[3,9], Stefan

8 Pöhlmann[1,2,11,*]

9

10 *[1]Infection Biology Unit, German Primate Center, Göttingen, Germany*

11 *[2]Faculty of Biology and Psychology, Georg-August-University Göttingen, Göttingen, Germany*

12 *[3]Institute of Molecular Virology, Ulm University Medical Center, Ulm, Germany*

13 *[4]Junior Research Group Herpesviruses - Infection Biology Unit, German Primate Center,*

14 *Göttingen, Germany*

15 *[5]Department of Anaesthesiology, University of Göttingen Medical Center, Göttingen, Georg-*

16 *August University of Göttingen, Robert-Koch-Str. 40, 37075 Göttingen, Germany*

17 *[6]Division of Molecular Immunology, Department of Internal Medicine 3, Friedrich-Alexander*

18 *University of Erlangen-Nürnberg, Erlangen, Germany*

19 *[7]Department of Transfusion Medicine, Ulm University, Ulm, Germany and Institute for Clinical*

20 *Transfusion Medicine and Immunogenetics, German Red Cross Blood Transfusion Service*

21 *Baden-Württemberg – Hessen and University Hospital Ulm, Ulm, Germany*

22 *[8]Department of Internal Medicine 1, Ulm University Hospital, Ulm, Germany*

23 *[9]Core Facility Functional Peptidomics, Ulm University Medical Center, Ulm, Germany*

24

25 [10]These authors contributed equally

26 [11]Lead contact

27 *Correspondence: mhoffmann@dpz.eu (M.H.), spoehlmann@dpz.eu (S.P.)

SUMMARY

The global spread of SARS-CoV-2/COVID-19 is devastating health systems and economies worldwide. Recombinant or vaccine-induced neutralizing antibodies are used to combat the COVID-19 pandemic. However, recently emerged SARS-CoV-2 variants B.1.1.7 (UK), B.1.351 (South Africa) and B.1.1.248 (Brazil) harbor mutations in the viral spike (S) protein that may alter virus-host cell interactions and confer resistance to inhibitors and antibodies. Here, using pseudoparticles, we show that entry of UK, South Africa and Brazil variant into human cells is susceptible to blockade by entry inhibitors. In contrast, entry of the South Africa and Brazil variant was partially (Casirivimab) or fully (Bamlanivimab) resistant to antibodies used for COVID-19 treatment and was less efficiently inhibited by serum/plasma from convalescent or BNT162b2 vaccinated individuals. These results suggest that SARS-CoV-2 may escape antibody responses, which has important implications for efforts to contain the pandemic.

2

52 **INTRODUCTION**

53 The pandemic spread of severe acute respiratory syndrome coronavirus 2 (SARS-CoV-2), the

54 causative agent of coronavirus disease 2019 (COVID-19), is ravaging economies and health

55 system worldwide and has caused more than 2.3 million deaths ((WHO), 2020). The

56 identification of antivirals by drug repurposing was so far largely unsuccessful. Remdesivir, an

57 inhibitor of the viral polymerase, is the only antiviral with proven efficacy (Beigel et al., 2020).

58 However, the clinical benefit reported for Remdesivir treatment is moderate and has been called

59 into question (Consortium et al., 2020; Wang et al., 2020). Recombinant antibodies, which target

60 the viral spike protein (S) and neutralize infection in cell culture and animal models (Baum et al.,

61 2020a; Chen et al., 2020), have been granted emergency use authorization (EUA) and may

62 provide a valuable treatment option in the absence of other antivirals. In contrast to the moderate

63 success in the area of antivirals, protective mRNA- and vector-based vaccines encoding the

64 SARS-CoV-2 S protein have been approved for human use and are considered key to the

65 containment of COVID-19 (Baden et al., 2021; Polack et al., 2020).

66   SARS-CoV-2, an enveloped, positive-strand RNA virus that uses its envelope protein

67 spike (S) to enter target cells. Entry depends on S protein binding to the cellular receptor ACE2

68 and S protein priming by the cellular serine protease TMPRSS2 (Hoffmann et al., 2020b; Zhou et

69 al., 2020) and these processes can be disrupted by soluble ACE2 and serine protease inhibitors

70 (Hoffmann et al., 2020b; Monteil et al., 2020; Zhou et al., 2020). Further, the S protein of SARS-

71 CoV-2 and other coronaviruses is a major determinant of viral cell and species tropism and the

72 main target for the neutralizing antibody response. The genetic information of SARS-CoV-2 has

73 remained relatively stable after the detection of first cases in Wuhan, China, in the winter season

74 of 2019. The only exception was a D614G change in the viral S protein that became dominant

75 early in the pandemic and that has been associated with increased transmissibility (Korber et al.,

3

76   2020; Plante et al., 2020; Volz et al., 2021). In contrast, D614G has only a moderate impact on

77   SARS-CoV-2 neutralization by sera from COVID-19 patients and by sera from vaccinated

78   individuals (Korber et al., 2020; Weissman et al., 2021).

79   In recent weeks several SARS-CoV-2 variants emerged that seem to exhibit increased

80   transmissibility and that harbor mutations in the S protein. The SARS-CoV-2 variant B.1.1.7 (UK

81   variant), also termed variant of concern (VOC) 202012/01 or 20I/501Y.V1, emerged in the

82   United Kingdom and was associated with a surge of COVID-19 cases (Leung et al., 2021).

83   Subsequently, spread of the UK variant in other countries was reported (Claro et al., 2021;

84   Galloway et al., 2021). It harbors nine mutations in the S protein, six of which are located in the

85   surface unit, S1, and three are found in the transmembrane unit, S2 (Fig. 1). Exchange N501Y is

86   located in the receptor binding domain (RBD), a domain within S1 that interacts with ACE2, and

87   its presence was linked to increased human-human transmissibility (Leung et al., 2021; Zhao et

88   al., 2021). Variants B.1.351 (20H/501Y.V2, also termed South Africa variant) and B.1.1.248

89   (P.1., also termed Brazil variant) were also purported to be more transmissible and these variants

90   harbor nine and eleven mutations in their S proteins, respectively, including three changes in the

91   RBD, K417N/T, E484K and N501Y (Fig. 1) (CDC, 2021). These mutations, as well as the

92   N501Y change present in the S protein of the UK variant, may alter host cell interactions and

93   susceptibility to experimental entry inhibitors and antibody-mediated neutralization. However, no

94   functional characterization of the S proteins of UK, South Africa and Brazil variant have been

95   reported in the peer-reviewed literature, with the exception of one study showing that the UK

96   variant exhibits reduced susceptibility to neutralization by sera from COVID-19 patients and

97   vaccinated individuals (Muik et al., 2021) and another study showing that mutations E484K and

98   N501Y, which are both present in the South Africa and Brazil variants, have little effect on

4

99   neutralization by sera from individuals who were immunized twice with BNT162b2 (Xie et al.,

100   2021).

101   Here, we show that the S protein of the UK, South Africa and Brazil variants mediate

102   robust entry into human cell lines and that entry is blocked by soluble ACE2 (sACE2), protease

103   inhibitors active against TMPRSS2 and membrane fusion inhibitors. In contrast, monoclonal

104   antibodies with EUA for COVID-19 treatment partially or completely failed to inhibit entry

105   driven by the S proteins of the South Africa and Brazil variants. Similarly, these variants were

106   less efficiently inhibited by convalescent plasma and sera from individuals vaccinated with

107   BNT162b2. Our results suggest that SARS-CoV-2 can evade inhibition by neutralizing

108   antibodies.

109

110

111

112

113

114

115

116

117

118

119

120

121

122

123   **RESULTS**

124

125   **The spike proteins of the SARS-CoV-2 variants mediate robust entry into human cell lines**

126   We first investigated whether the S proteins of SARS-CoV-2 WT (Wuhan-1 isolate with D614G

127   exchange), UK, South Africa and Brazil variants (Fig. 1) mediated entry into human and non-

128   human primate (NHP) cell lines with comparable efficiency. For this, we used a vesicular

129   stomatitis virus (VSV)-based vector pseudotyped with the respective S proteins. This system

130   faithfully mimics key aspects of SARS-CoV-2 entry into cells, including ACE2 engagement,

131   priming of the S protein by TMPRSS2 and antibody-mediated neutralization (Hoffmann et al.,

132   2020b). The following cell lines are frequently used for SARS-CoV-2 research and were

133   employed as target cells in our study: The African green monkey kidney cell line Vero, Vero

134   cells engineered to express TMPRSS2, the human embryonic kidney cell line 293T, 293T cells

135   engineered to express ACE2, the human lung cell line Calu-3 and the human colon cell line

136   Caco-2. All cell lines tested express endogenous ACE2. In addition, Calu-3 and Caco-2 cells

137   express endogenous TMPRSS2 (Bottcher-Friebertshauser et al., 2011; Kleine-Weber et al.,

138   2018).

139   All S proteins studied were robustly expressed and mediated formation of syncytia in

140   transfected cells (Fig. 2A). Entry into all cell lines was readily detectable but the relative entry

141   efficiency varied. Particles bearing the S proteins of the SARS-CoV-2 variants entered 293T

142   (Brazil variant) and 293T-ACE2 (South Africa and Brazil variants) cells with slightly reduced

143   efficiency as compared to particles bearing WT S protein, while the reverse observation was

144   made for Calu-3 cells (UK variant). For the remaining cell lines, no significant differences in

145   entry efficiency were observed between SARS-CoV S WT and S proteins from SARS-CoV-2

6

146   variants (Fig. 2B). Collectively, these results indicate that the mutations present in the S proteins

147   of UK, South Africa and Brazil variant are compatible with robust entry into human cells.

148

149   **The spike proteins of the SARS-CoV-2 variants mediate fusion of human cells**

150   The S protein of SARS-CoV-2 drives cell-cell fusion resulting in the formation of syncytia and

151   this process might contribute to viral pathogenesis (Buchrieser et al., 2021). We employed a cell-

152   cell fusion assay to determine whether the S proteins of UK, South Africa and Brazil variant

153   drive fusion with human cells. For this, the S proteins under study were expressed in effector

154   293T cells, which were subsequently mixed with target 293T cells engineered to express ACE2

155   or ACE2 in conjunction with TMPRSS2. The S protein of SARS-CoV was included as control.

156   The SARS-CoV S protein failed to mediate fusion with target cells expressing ACE2 only but

157   efficiently drove fusion with cells expressing ACE2 and TMPRSS2 (Fig. 3A). Similar results

158   were obtained by microscopic examination of A549-ACE2 and A549-ACE2/TMPRSS2 cells

159   transfected to express the respective S proteins (Fig. 3B). These findings are in agreement with

160   the documented requirement for an exogenous protease for SARS-CoV S driven cell-cell fusion

161   under the experimental conditions chosen (Hoffmann et al., 2020a). In contrast, the SARS-CoV-2

162   S protein mediated efficient membrane fusion in the absence of TMPRSS2 expression in target

163   cells (Fig. 3A,B) and this property is known to depend on the multibasic S1/S2 site of this S

164   protein which is absent in SARS-CoV S (Hoffmann et al., 2020a). Finally, the S proteins of all

165   SARS-CoV-2 variants tested facilitated cell-cell fusion with similar (UK) or slightly reduced

166   (South Africa, Brazil) efficiency as compared to WT S protein (Fig. 3A,B).

167

168   **Similar stability and entry kinetics of particles bearing WT and variant S proteins**

169   We next investigated whether the S proteins of the SARS-CoV-2 variants showed altered

170   stability, which may contribute to the alleged increased transmissibility of the viral variants. For

171   this, we incubated S protein-bearing particles for different time intervals at 33°C, a temperature

172   that is present in the nasal cavity, and subsequently assessed their capacity to enter target cells.

173   The efficiency of cell entry markedly decreased upon incubation of particles at 33°C for more

174   than 8 h, but no appreciable differences were observed between particles bearing S proteins from

175   SARS-CoV-2 WT or variants (Fig. 4A).

176   Although the S proteins of the SARS-CoV-2 variants under study did not differ markedly

177   from WT S protein regarding stability and entry efficiency, they might mediate entry with

178   different kinetics as compared to WT S protein. To investigate this possibility, we incubated

179   target cells with S protein-bearing particles for the indicated time intervals, removed unbound

180   virus by washing and universally determined entry efficiency at 16 h post inoculation. Entry

181   efficiency increased with the time available for particle adsorption to cells but no clear

182   differences were observed between particles bearing WT S protein or S protein from SARS-CoV-

183   2 variants (Fig. 4B). Our results suggest that there might be no major differences between WT

184   SARS-CoV-2 and SARS-CoV-2 variants UK, South Africa and Brazil regarding S protein

185   stability and entry kinetics.

186

187   **Soluble ACE2, TMPRSS2 inhibitors and membrane fusion inhibitors block entry**

188   Soluble ACE2 (sACE2) blocks SARS-CoV-2 entry into cells and is in clinical development for

189   COVID-19 therapy (Monteil et al., 2020). Similarly, the clinically proven protease inhibitors

190   Camostat and Nafamostat block TMPRSS2-dependent SARS-CoV-2 cell entry and their potential

191   for COVID-19 treatment is currently being assessed (Hoffmann et al., 2020b; Hoffmann et al.,

192   2020c). Finally, the membrane fusion inhibitor EK1 and its optimized lipid-conjugated derivative

193   EK1C4 block SARS-CoV-2 entry by preventing conformational rearrangements in S protein

194   required for membrane fusion (Xia et al., 2020). We asked whether entry driven by the S proteins

195   of UK, South Africa and Brazil variant can be blocked by these inhibitors. All inhibitors were

196   found to be active although entry mediated by the S proteins of the SARS-CoV-2 variants was

197   slightly more sensitive to blockade by sACE2 as compared to WT S protein, at least for certain

198   sACE2 concentrations (Fig. 5). Conversely, entry driven by the S protein of the Brazil variant

199   was slightly more sensitive to blockade by EK1 and EK1C4 as compared to the other S proteins

200   tested (Fig. 5). These results suggest that sACE2, TMPRSS2 inhibitors and membrane fusion

201   inhibitors will be active against UK, South Africa and Brazil variant.

202

203   **Resistance against antibodies used for COVID-19 treatment**

204   A cocktail of monoclonal antibodies (REGN-COV2, Casirivimab and Imdevimab) and the

205   monoclonal antibody Bamlanivimab block SARS-CoV-2 WT infection and have received EUA

206   for COVID-19 therapy. We analyzed whether these antibodies can inhibit entry driven by the S

207   proteins of UK, South Africa and Brazil variants. All variants were comparably inhibited by

208   antibody REGN10987 (Imdevimab) (Fig. 6). In contrast, entry driven by the S proteins of the

209   South Africa and Brazil variant was partially resistant against antibody REGN10933

210   (Casirivimab) and fully resistant against REGN10989 (Fig. 6). Finally, entry mediated by the S

211   proteins of the South Africa and Brazil variant was completely resistant to Bamlanivimab while

212   the S protein of the UK variant was efficiently blocked by all antibodies tested (Fig. 6).

213   Collectively, these data indicate that antibodies with EUA might provide incomplete

214   (REGENERON) or no (Bamlanivimab) protection against the South Africa and Brazil variants.

215

216   **Reduced neutralization by plasma from convalescent patients**

9

217   SARS-CoV-2 infection can induce the production of neutralizing antibodies and these antibodies

218   are believed to contribute to protection from reinfection (Rodda et al., 2020; Wajnberg et al.,

219   2020). Therefore, it is important to elucidate whether UK, South Africa and Brazil variants are

220   efficiently neutralized by antibody responses in convalescent COVID-19 patients. We addressed

221   this question using plasma collected from COVID-19 patients undergoing intensive care at

222   Göttingen University Hospital, Germany. The plasma samples had been pre-screened for high

223   neutralizing activity against WT S protein, and a plasma sample with no neutralizing activity was

224   included as negative control. Spread of SARS-CoV-2 variants in Germany was very limited at the

225   time of sample collection, indicating that serum antibodies were induced in response to SARS-

226   CoV-2 WT infection.

227   All plasma samples with known neutralizing activity (ID15, 18, 20, 22, 23, 24, 27, 33, 51)

228   efficiently reduced entry driven by WT S protein while the control plasma (ID16) was inactive

229   (Fig. 7A). Blockade of entry driven by the S protein of the UK variant was slightly less efficient

230   (Fig. 7A and C). In contrast, seven out of nine plasma samples inhibited entry driven by the S

231   proteins of the South Africa and Brazil variants less efficiently as compared to entry driven by

232   WT S protein. These results suggest that individuals previously infected with WT SARS-CoV-2

233   might only be partially protected against infection with South Africa and Brazil variants of

234   SARS-CoV-2.

235

236   **Reduced neutralization by sera from BNT162b2-vaccinated individuals**

237   The vaccine BNT162b2 is based on an mRNA that encodes for the viral S protein and is highly

238   protective against COVID-19 (Polack et al., 2020). While the S protein harbor T-cell epitopes

239   (Grifoni et al., 2020; Peng et al., 2020), efficient protection is believed to require the induction of

240   neutralizing antibodies. We determined neutralizing activity of sera from 15 donors immunized

10

241   twice with BNT162b2 (Table S1). All sera efficiently inhibited entry driven by the WT S protein

242   and inhibition of entry driven by the S protein of the UK variant was only slightly reduced (Fig.

243   7B,C). In contrast, 12 out of 15 sera showed a markedly reduced inhibition of entry driven by the

244   S proteins of the South Africa and Brazil variant (Fig. 7B,C), although it should be stated that all

245   sera completely inhibited entry at the lowest dilution tested. In sum, these results suggest that

246   BNT162b2 may offer less robust protection against infection by these variants as compared to

247   SARS-CoV-2 WT.

248

249

250

251

252

253

254

255

256

257

258

259

260

261

262

263

264

265   **DISCUSSION**

266   The COVID-19 pandemic has taken a major toll on human health and prosperity. Non-

267   pharmaceutic interventions are currently the major instrument to combat the pandemic but are

268   associated with a heavy burden on economies. Protective vaccines became recently available and

269   might become a game changer – it is hoped that efficient vaccine roll out might allow to attain

270   herd immunity in certain countries in the second half of 2021. The recent emergence of SARS-

271   CoV-2 variants UK, South Africa and Brazil that harbor mutations in the major target of

272   neutralizing antibodies, the viral S protein, raises the question whether vaccines available at

273   present will protect against infection with these viruses. Similarly, it is largely unclear whether

274   antibody responses in convalescent patients protect against re-infection with the new variants.

275   The results of the present study suggest that SARS-CoV-2 variants South Africa and Brazil are

276   partially (Casirivimab) or fully (Bamlanivimab) resistant against antibodies used for COVID-19

277   treatment and are inhibited less efficiently by convalescent plasma or sera from individuals

278   immunized with the mRNA vaccine BNT162b2. These results suggest that strategies relying on

279   antibody-mediated control of SARS-CoV-2 infection might be compromised by resistance

280   development.

281   The increased transmissibility postulated for the UK variant and purported for the South

282   Africa and Brazil variants suggest that these viruses might exhibit altered host-cell interactions or

283   stability. The present analysis suggests that there are no major differences in host cell entry of

284   WT SARS-CoV-2 and the UK, South Africa and Brazil variant (CDC, 2021; Leung et al., 2021).

285   Thus, the S proteins of these viruses mediated entry into various cell lines with roughly

286   comparable efficiency and no evidence for increased S protein stability or differences in entry

287   kinetics were obtained. Similarly, the S proteins of all variants were able to mediate fusion of

288   human cells. Moreover, entry driven by all S proteins studied was blocked by sACE2, protease

12

289   inhibitors targeting TMPRSS2 and a membrane fusion inhibitor. However, it should be noted that

290   the S proteins of all variants were slightly more susceptible to blockade by sACE2, suggesting

291   differences in ACE2 engagement between WT and variant S proteins.

292   Although host-cell interactions underlying viral entry might not differ markedly between

293   SARS-CoV-2 S protein WT and the variants studied here, major differences in susceptibility to

294   antibody-mediated neutralization were observed. Entry driven by the S proteins of the South

295   Africa and Brazil variants was not inhibited by one of the REGENERON antibodies

296   (REGN10989) and Bamlanivimab (Baum et al., 2020a; Baum et al., 2020b; Chen et al., 2020;

297   Gottlieb et al., 2021), suggesting that these antibodies might not be suitable for treatment of

298   COVID-19 patients infected with these variants. The partial resistance against Casirivimab

299   (REGN10933) is in keeping with mutations present in the S protein of South Africa and Brazil

300   variant being located at the antibody binding site (Fig. S1). Moreover, and more importantly,

301   entry driven by the S proteins of the South Africa and Brazil variants were markedly less

302   sensitive to neutralization by antibodies from convalescent patients and vaccinated individuals as

303   compared to the WT S protein. It should be noted that all plasma and sera tested completely

304   inhibited entry at the lowest dilution tested and that T cell responses will contribute to control of

305   SARS-CoV-2 infection, particularly in re-infected convalescent patients (Grifoni et al., 2020;

306   Peng et al., 2020). Nevertheless, the markedly reduced sensitivity to antibody-mediated

307   neutralization suggests that convalescent and vaccinated individuals might not be fully protected

308   against infection by the South Africa and Brazil variants. Such a scenario would be in keeping

309   with preliminary information suggesting that certain vaccines might provide less effective

310   protection in South African as compared to the US (Callaway and Mallapaty, 2021). On a more

311   general level, our findings suggest that the interface between the SARS-CoV-2 S protein and

312   ACE2 exhibits high plasticity, favoring emergence of escape variants.

13

313   Our find that entry driven by the S protein of the UK variant can be efficiently inhibited

314   by antibodies induced upon infection and vaccination is in agreement with those of Muik and

315   colleagues, who reported that pseudoparticles bearing the UK S protein are efficiently neutralized

316   by sera from BNT162b2 vaccinated individuals (Muik et al., 2021). Xie and coworkers found that

317   authentic SARS-CoV-2 bearing two mutations present in the S protein of the UK variant (69/70-

318   deletion + N501Y) was still robustly neutralized by antibodies induced by vaccination with

319   BNT162b2, again in keeping with our findings. Neutralization of a virus bearing two changes

320   found in the S protein of the South Africa variant (E484K + N501Y) was moderately reduced and

321   it is conceivable that neutralization resistance would have been further increased by the other four

322   mutations present in the S1 unit of the S protein of the South Africa variant, including K417N,

323   which is located in the RBD (Xie et al., 2021).

324   Our results await confirmation with authentic SARS-CoV-2. However, the data available

325   at present suggest that the South Africa and Brazil variants constitute an elevated threat to human

326   health and that containment of these variants by non-pharmaceutic interventions is an important

327   task.

328

329

330

331

332

333

334

335

336

14

337   **MATERIAL AND METHODS**

338

339   **Cell culture**

340   All cell lines were incubated at 37 °C in a humidified atmosphere containing 5% CO_2. All media

341   were supplemented with 10% fetal bovine serum (FCS, Biochrom or GIBCO), 100 U/ml of

342   penicillin and 0.1 mg/ml of streptomycin (PAN-Biotech). 293T (human, kidney; ACC-635,

343   DSMZ), 293T cells stably expressing ACE2 (293T-ACE2), BHK-21 (Syrian hamster, kidney

344   cells; CCL-10, ATCC), Vero76 (African green monkey, kidney; CRL-1586, ATCC; kindly

345   provided by Andrea Maisner, Institute of Virology, Philipps University Marburg, Marburg,

346   Germany) and Vero-TMPRSS2 cells (Hoffmann et al., 2020b) were cultivated in Dulbecco's

347   modified Eagle medium (DMEM). Vero-TMPRSS2 cells additionally received puromycin (0.5

348   µg/ml, Invivogen). A549 (human, lung; CRM-CCL-185, ATCC), A549-ACE2 and A549-

349   ACE2/TMPRSS2 cells were cultivated in DMEM/F-12 Medium with Nutrient Mix

350   (ThermoFisher Scientific). A549-ACE2 cells further received 0.5 µg/ml puromycin, while A549-

351   ACE2/TMPRSS2 cells were cultivated in the presence of 0.5 µg/ml puromycin and 1 µg/ml

352   blasticidin. Caco-2 (human, intestine; HTB-37, ATCC) and Calu-3 cells (human, lung; HTB-55,

353   ATCC; kindly provided by Stephan Ludwig, Institute of Virology, University of Münster,

354   Germany) were cultivated in minimum essential medium supplemented with 1x non-essential

355   amino acid solution (from 100x stock, PAA) and 1 mM sodium pyruvate (Thermo Fisher

356   Scientific). 293T cells that stably express ACE2 were generated by retroviral (murine leukemia

357   virus, MLV) transduction and selection of parental 293T cells with puromycin (4 µg/ml for initial

358   selection and 0.5 µg/ml for sub-culturing). Similarly, we generated A549 cells stably expressing

359   ACE2 (A549-ACE2). A549 cells stably expressing ACE2 and TMPRSS2 (A549-

360   ACE2/TMPRSS2) were obtained by retroviral transduction of A549-ACE2 cells and selection

361 with blasticidin (6 µg/ml for initial selection and 1 µg/ml for sub-culturing). Authentication of

362 cell lines was performed by STR-typing, amplification and sequencing of a fragment of the

363 cytochrome c oxidase gene, microscopic examination and/or according to their growth

364 characteristics. Further, cell lines were routinely tested for contamination by mycoplasma.

365 Transfection of cells was carried out by the calcium-phosphate method or by using

366 polyethylenimin, Lipofectamine LTX (Thermo Fisher Scientific) or Transit LT-1 (Mirus).

367

368 **Plasmids**

369 Expression plasmids for DsRed (PMID: 32142651), vesicular stomatitis virus (VSV, serotype

370 Indiana) glycoprotein (VSV-G) (Brinkmann et al., 2017), SARS-S (derived from the Frankfurt-1

371 isolate; containing a C-terminal HA epitope tag) (Hoffmann et al., 2020b), SARS-2-S (codon-

372 optimized, based on the Wuhan/Hu-1/2019 isolate; with a C-terminal truncation of 18 amino acid

373 residues or with a C-terminal HA epitope tag) (Hoffmann et al., 2020b), angiotensin-converting

374 enzyme 2 (ACE2) (Hoffmann et al., 2013), TMPRSS2 (Heurich et al., 2014) have been described

375 elsewhere. In order to generate expression vectors for S proteins from emerging SARS-CoV-2

376 variants, we introduced the required mutations into the parental SARS-2-S sequence by overlap

377 extension PCR. Subsequently, the respective open reading frames were inserted into the pCG1

378 plasmid (kindly provided by Roberto Cattaneo, Mayo Clinic College of Medicine, Rochester,

379 MN, USA), making use of the unique BamHI and XbaI restriction sites. Further, we cloned the

380 coding sequence for human ACE2 into the pQCXIP plasmid (Brass et al., 2009), yielding

381 pQCXIP_ACE2. For the generation of cell lines stably overexpressing human TMPRSS2 and/or

382 human ACE2 we produced MLV-based transduction vectors using the pQCXIBl_cMYC-

383 hTMPRSS2 (Kleine-Weber et al., 2018) or pQCXIP_ACE2 expression vectors in combination

384 with plasmids coding for VSV-G and MLV-Gag/Pol (Bartosch et al., 2003). In order to obtain the

385 expression vector for soluble human ACE2 harboring the Fc portion of human immunoglobulin

386 G (sol-ACE2-Fc), we PCR amplified the sequence coding for the ACE2 ectodomain (amino acid

387 residues 1-733) and cloned it into the pCG1-Fc plasmid ((Sauer et al., 2014), kindly provided by

388 Georg Herrler, University of Veterinary Medicine, Hannover, Germany). Sequence integrity was

389 verified by sequencing using a commercial sequencing service (Microsynth Seqlab). Specific

390 cloning details (e.g., primer sequences and restriction sites) are available upon request.

391

392 **Sequence analysis and protein models**

393 S protein sequences of emerging SARS-CoV-2 S variants found in the United Kingdom (UK,

394 EPI_ISL_601443), South Africa (SA, EPI_ISL_700428) and Brazil (BRA, EPI_ISL_792683)

395 were retrieved from the GISAID (global initiative on sharing all influenza data) database

396 (https://www.gisaid.org/). Protein models are based on PDB: 6XDG (Hansen et al., 2020) or a

397 template generated by modelling the SARS-2-S sequence on a published crystal structure (PDB:

398 6XR8,(Cai et al., 2020)), using the SWISS-MODEL online tool (https://swissmodel.expasy.org/),

399 and were generated using the YASARA software (http://www.yasara.org/index.html).

400

401 **Production of soluble ACE2 (sol-ACE2-Fc)**

402 293T cells were grown in a T-75 flask and transfected with 20 µg of sol-ACE2-Fc expression

403 plasmid. At 10 h posttransfection, the medium was replaced and cells were further incubated for

404 38 h before the culture supernatant was collected and centrifuged (2,000 x g, 10 min, 4 °C). Next,

405 the clarified supernatant was loaded onto Vivaspin protein concentrator columns with a

406 molecular weight cut-off of 30 kDa (Sartorius) and centrifuged at 4,000 x g, 4 °C until the sample

407 was concentrated by a factor of 20. The concentrated sol-ACE2-Fc was aliquoted and stored at -

408 80 °C until further use.

409

Collection of serum and plasma samples

Sera from individuals vaccinated with BioNTech/Pfizer vaccine BNT162b2 were obtained 13-15

days after the second dose. Study was approved by the Ethic committee of Ulm university (vote

31/21 – FSt/Sta). Collection of plasma samples from COVID-19 patients treated at the intensive

care unit was approved by the Ethic committee of the University Medicine Göttingen

(SeptImmun Study 25/4/19 Ü). For collection of plasma, Cell Preparation Tube (CPT)

vacutainers with sodium citrate were used and plasma was collected as supernatant over the

PBMC layer. For vaccinated patients, blood was collected in S-Monovette® Serum Gel tubes

(Sarstedt). Subsequently, the plasma and serum samples were incubated at 56°C for 30 min to

inactivate putative infectious virus and for reconvalescent plasma pre-screening for detection of

neutralizing activity was performed on Vero76 cells using SARS-2-S- and VSV-G bearing

pseudotypes as control, normalized for equal infectivity.

Pseudotyping of VSV and transduction experiments

Rhabdoviral pseudotype particles were prepared according to a published protocol (Kleine-

Weber et al., 2019). For pseudotyping we used a replication-deficient VSV vector that lacks the

genetic information for VSV-G and instead codes for two reporter proteins, enhanced green

fluorescent protein and firefly luciferase (FLuc), VSV*ΔG-FLuc (kindly provided by Gert

Zimmer, Institute of Virology and Immunology, Mittelhäusern, Switzerland) (Berger Rentsch and

Zimmer, 2011). 293T cells transfected to express the desired viral glycoprotein were inoculated

with VSV*ΔG-FLuc and incubated for 1 h at 37 °C before the inoculum was removed and cells

were washed. Finally, culture medium containing anti-VSV-G antibody (culture supernatant from

I1-hybridoma cells; ATCC no. CRL-2700) was added. Following an incubation period of 16-18

18

433   h, pseudotype particles were harvested by collecting the culture supernatant, pelleting cellular

434   debris through centrifugation (2,000 x g, 10 min, room temperature) and transferring aliquots of

435   the clarified supernatant into fresh reaction tubes. Samples were stored at -80 °C. For

436   transduction experiments, target cells were seeded in 96-well plates, inoculated with the

437   respective pseudotype particles with comparable infectivity and further incubated. At 16-18 h

438   postinoculation, transduction efficiency was analyzed. For this, the culture supernatant was

439   removed and cells were lysed by incubation for 30 min at room temperature with Cell Culture

440   Lysis Reagent (Promega). Next, lysates were transferred into white 96-well plates and FLuc

441   activity was measured using a commercial substrate (Beetle-Juice, PJK; Luciferase Assay

442   System, Promega) and a plate luminometer (Hidex Sense Plate Reader, Hidex or Orion II

443   Microplate Luminometer, Berthold)..

444   Depending on the experimental set-up target cells were either transfected in advance (24

445   h) with ACE2 expression plasmid or empty vector (BHK-21), or pre-incubated with different

446   concentrations of serine protease inhibitor (Camostat or Nafamostat, Caco-2, 1 h at 37 °C).

447   Alternatively, pseudotype particles were pre-incubated with different concentrations of either sol-

448   ACE2-Fc, fusion inhibitor (EK-1 or EK-1-C4), monoclonal antibodies (REGN10933,

449   REGN10987, REGN10989, Bamlaivimab/LY-CoV555), or sera from COVID-19 patients or

450   vaccinated (Pfizer/BioNTech vaccine BNT162b2) individuals (30 min at 37 °C). S protein

451   stability was analyzed as follows, pseudotype particles were incubated for different time intervals

452   at 33 °C the snap-frozen and stored at -80 °C until all samples were collected. Thereafter,

453   samples were thawed and inoculated onto Vero76 cells and incubated as described above. For the

454   investigation of the entry speed of S protein-bearing pseudotypes, the respective particles were

455   inoculated on Vero76 cells and adsorbed for different time intervals before the inoculum was

456   removed and cells were washed and incubated with fresh medium.

457

Analysis of S protein expression by fluorescence microscopy

A549-ACE2 cells that were grown on coverslips were transfected with plasmids encoding SARS-CoV-2 S protein variants with a C-terminal HA epitope tag or empty expression vector (control). At 24 h posttransfection, cells were fixed with 4 % paraformaldehyde solution (30 min, room temperature), washed and incubated (15 min, room temperature) with phosphate-buffered saline (PBS) containing 0.1 M glycine and permeabilized by treatment with 0.2 % Triton-X-100 solution (in PBS, 15 min). Thereafter, samples were washed and incubated for 1 h at room temperature with primary antibody (anti-HA, mouse, 1:500, Sigma-Aldrich) diluted in PBS containing 1 % bovine serum albumin. Next, the samples were washed with PBS and incubated in the dark for 1 h at 4 °C with secondary antibody (Alexa Fluor-568-conjugated anti-mouse antibody, 1:750, Thermo Fisher Scientific). Finally, the samples were washed, nuclei were stained with DAPI and coverslips were mounted onto microscopic glass slides with Mowiol/DABCO. Images were taken using a Zeiss LSM800 confocal laser scanning microscope with ZEN imaging software (Zeiss).

472

Qualitative cell-cell fusion assay

A549-ACE2 or A549-ACE2/TMPRSS2 cells were transfected with DsRed expression plasmid along with either expression vector for wildtype or mutant SARS-2-S, SARS-S or empty plasmid. At 24 h posttransfection, cells were fixed with 4 % paraformaldehyde solution (30 min, room temperature), washed and nuclei were stained with DAPI. Next, cells were washed again with PBS and images were taken using a Zeiss LSM800 confocal laser scanning microscope with ZEN imaging software (Zeiss).

480

20

Quantitative cell-cell fusion assay

293T target-cells were seeded in a 48-well plate at 50.000 cells/well and transfected with Gal4-

TurboGFP-Luciferase expression plasmid (Gal4-TurboGFP-Luc) as well as expression plasmid

for ACE2 alone or in combination with TMPRSS2 (5:1 ratio). 293T effector-cells were seeded in

a 10 cm dish at 70-80% confluency and transfected with the Vp16-Gal4 expression plasmid as

well as expression plasmid for WT or mutant SARS-2-S, SARS-S or empty plasmid. At 24h

posttransfection, effector-cells were detached by resuspending them in culture medium and added

to the target-cells in a 1:1 ratio. After 24-48 h luciferase activity was analyzed using the

PromoKine Firefly Luciferase Kit or Beetle-Juice Luciferase Assay according to manufacturer's

instructions and a Biotek Synergy 2 plate reader.

Data normalization and statistical analysis

Data analysis was performed using Microsoft Excel as part of the Microsoft Office software

package (version 2019, Microsoft Corporation) and GraphPad Prism 8 version 8.4.3 (GraphPad

Software). Data normalization was done as follows: (i) To compare efficiency of cell entry driven

by the different S protein variants under study, transduction was normalized against SARS-CoV-

2 S WT (set as 100%); (ii) For experiments investigating inhibitory effects, transduction was

normalized against a reference sample (e.g., control-treated cells or pseudotypes, set as 100%).

Serum dilutions the cause a 50 % reduction of transduction efficiency (neutralizing titer 50,

NT50), were calculated using a non-linear regression model (inhibitor vs. normalized response,

variable slope). Statistical significance was tested by one- or two-way analysis of variance

(ANOVA) with Dunnett's or Sidak's post-hoc test, or by paired student`s t-test. Only P values of

0.05 or lower were considered statistically significant (P > 0.05, not significant [ns]; P ≤ 0.05, *;

21

504    $P \leq 0.01$, **; $P \leq 0.001$, ***). Specific details on the statistical test and the error bars are

505   indicated in the figure legends.

506

507

508

509

510

511

512

513

514

515

516

517

518

519

520

521

522

523

524

525

526

527

528   **SUPPLEMENTAL INFORMATION**

529

530   **Fígure S1.** Location of SARS-2-S RBD mutations K417N/T, E484K and N501Y with respect to

531   the binding interface of the REGN-COV2 antibody cocktail (related to Figure 6).

532   The protein models of the SARS-2-S receptor-binding domain (RBD, blue) in complex with

533   antibodies Casirivimab (REGN10933, orange) and Imdevimab (REGN10987, green) were

534   constructed based on the 6XDG template (Hansen et al., 2020). Residues highlighted in red

535   indicate amino acid variations found in emerging SARS-CoV-2 variants from the United

536   Kingdom, South Africa and Brazil.

537

553

554   **AUTHOR CONTRIBUTIONS**

555   Conceptualization, M.H., J.M., S.P.; Funding acquisition, S.P., J.M.; Investigation, M.H., P.A.,

556   R.G., A.S., B.H., A.H., N.K., L.G., H.H.-W., A.K., Essential resources, M.S.W., S.S., H.-M.J.,

557   B.J., H.S., M.M., A.K.; Writing, M.H. and S.P., Review and editing, all authors.

558

559   **DECLARATION OF INTEREST**

560   The authors declare not competing interests

561

562

563

564

565

566

567

568

569

570

571

572

573

574

REFERENCES

(WHO), W.H.O. (2020). Weekly epidemiological update - 9 February 2021 (WHO).

Baden, L.R., El Sahly, H.M., Essink, B., Kotloff, K., Frey, S., Novak, R., Diemert, D., Spector, S.A., Rouphael, N., Creech, C.B.*, et al.* (2021). Efficacy and Safety of the mRNA-1273 SARS-CoV-2 Vaccine. N Engl J Med *384*, 403-416.

Bartosch, B., Dubuisson, J., and Cosset, F.L. (2003). Infectious hepatitis C virus pseudo-particles containing functional E1-E2 envelope protein complexes. J Exp Med *197*, 633-642.

Baum, A., Ajithdoss, D., Copin, R., Zhou, A., Lanza, K., Negron, N., Ni, M., Wei, Y., Mohammadi, K., Musser, B.*, et al.* (2020a). REGN-COV2 antibodies prevent and treat SARS-CoV-2 infection in rhesus macaques and hamsters. Science *370*, 1110-1115.

Baum, A., Fulton, B.O., Wloga, E., Copin, R., Pascal, K.E., Russo, V., Giordano, S., Lanza, K., Negron, N., Ni, M.*, et al.* (2020b). Antibody cocktail to SARS-CoV-2 spike protein prevents rapid mutational escape seen with individual antibodies. Science *369*, 1014-1018.

Beigel, J.H., Tomashek, K.M., Dodd, L.E., Mehta, A.K., Zingman, B.S., Kalil, A.C., Hohmann, E., Chu, H.Y., Luetkemeyer, A., Kline, S.*, et al.* (2020). Remdesivir for the Treatment of Covid-19 - Preliminary Report. N Engl J Med.

Berger Rentsch, M., and Zimmer, G. (2011). A vesicular stomatitis virus replicon-based bioassay for the rapid and sensitive determination of multi-species type I interferon. PLoS One *6*, e25858.

Bottcher-Friebertshauser, E., Stein, D.A., Klenk, H.D., and Garten, W. (2011). Inhibition of influenza virus infection in human airway cell cultures by an antisense peptide-conjugated morpholino oligomer targeting the hemagglutinin-activating protease TMPRSS2. J Virol *85*, 1554-1562.

Brass, A.L., Huang, I.C., Benita, Y., John, S.P., Krishnan, M.N., Feeley, E.M., Ryan, B.J., Weyer, J.L., van der Weyden, L., Fikrig, E.*, et al.* (2009). The IFITM proteins mediate cellular resistance to influenza A H1N1 virus, West Nile virus, and dengue virus. Cell *139*, 1243-1254.

Brinkmann, C., Hoffmann, M., Lubke, A., Nehlmeier, I., Kramer-Kuhl, A., Winkler, M., and Pohlmann, S. (2017). The glycoprotein of vesicular stomatitis virus promotes release of virus-like particles from tetherin-positive cells. PLoS One *12*, e0189073.

Buchrieser, J., Dufloo, J., Hubert, M., Monel, B., Planas, D., Rajah, M.M., Planchais, C., Porrot, F., Guivel-Benhassine, F., Van der Werf, S.*, et al.* (2021). Syncytia formation by SARS-CoV-2-infected cells. EMBO J *40*, e107405.

Cai, Y., Zhang, J., Xiao, T., Peng, H., Sterling, S.M., Walsh, R.M., Jr., Rawson, S., Rits-Volloch, S., and Chen, B. (2020). Distinct conformational states of SARS-CoV-2 spike protein. Science *369*, 1586-1592.

Callaway, E., and Mallapaty, S. (2021). Novavax offers first evidence that COVID vaccines protect people against variants. Nature *590*, 17.

CDC, C.f.D.C.a.P. (2021). Emerging SARS-CoV-2 Variants.

Chen, P., Nirula, A., Heller, B., Gottlieb, R.L., Boscia, J., Morris, J., Huhn, G., Cardona, J., Mocherla, B., Stosor, V.*, et al.* (2020). SARS-CoV-2 Neutralizing Antibody LY-CoV555 in Outpatients with Covid-19. N Engl J Med.

Claro, I.M., da Silva Sales, F.C., Ramundo, M.S., Candido, D.S., Silva, C.A.M., de Jesus, J.G., Manuli, E.R., de Oliveira, C.M., Scarpelli, L., Campana, G.*, et al.* (2021). Local Transmission of SARS-CoV-2 Lineage B.1.1.7, Brazil, December 2020. Emerg Infect Dis *27*.

Consortium, W.H.O.S.T., Pan, H., Peto, R., Henao-Restrepo, A.M., Preziosi, M.P., Sathiyamoorthy, V., Abdool Karim, Q., Alejandria, M.M., Hernandez Garcia, C., Kieny, M.P.*, et al.* (2020). Repurposed Antiviral Drugs for Covid-19 - Interim WHO Solidarity Trial Results. N Engl J Med.

Galloway, S.E., Paul, P., MacCannell, D.R., Johansson, M.A., Brooks, J.T., MacNeil, A., Slayton, R.B., Tong, S., Silk, B.J., Armstrong, G.L.*, et al.* (2021). Emergence of SARS-CoV-2 B.1.1.7 Lineage - United States, December 29, 2020-January 12, 2021. MMWR Morb Mortal Wkly Rep *70*, 95-99.

Gottlieb, R.L., Nirula, A., Chen, P., Boscia, J., Heller, B., Morris, J., Huhn, G., Cardona, J., Mocherla, B., Stosor, V.*, et al.* (2021). Effect of Bamlanivimab as Monotherapy or in Combination With Etesevimab on Viral Load in Patients With Mild to Moderate COVID-19: A Randomized Clinical Trial. JAMA.

Grifoni, A., Weiskopf, D., Ramirez, S.I., Mateus, J., Dan, J.M., Moderbacher, C.R., Rawlings, S.A., Sutherland, A., Premkumar, L., Jadi, R.S.*, et al.* (2020). Targets of T Cell Responses to SARS-CoV-2 Coronavirus in Humans with COVID-19 Disease and Unexposed Individuals. Cell *181*, 1489-1501 e1415.

Hansen, J., Baum, A., Pascal, K.E., Russo, V., Giordano, S., Wloga, E., Fulton, B.O., Yan, Y., Koon, K., Patel, K.*, et al.* (2020). Studies in humanized mice and convalescent humans yield a SARS-CoV-2 antibody cocktail. Science *369*, 1010-1014.

Heurich, A., Hofmann-Winkler, H., Gierer, S., Liepold, T., Jahn, O., and Pohlmann, S. (2014). TMPRSS2 and ADAM17 cleave ACE2 differentially and only proteolysis by TMPRSS2 augments entry driven by the severe acute respiratory syndrome coronavirus spike protein. J Virol *88*, 1293-1307.

Hoffmann, M., Kleine-Weber, H., and Pohlmann, S. (2020a). A Multibasic Cleavage Site in the Spike Protein of SARS-CoV-2 Is Essential for Infection of Human Lung Cells. Mol Cell *78*, 779-784 e775.

Hoffmann, M., Kleine-Weber, H., Schroeder, S., Kruger, N., Herrler, T., Erichsen, S., Schiergens, T.S., Herrler, G., Wu, N.H., Nitsche, A.*, et al.* (2020b). SARS-CoV-2 Cell Entry Depends on ACE2 and TMPRSS2 and Is Blocked by a Clinically Proven Protease Inhibitor. Cell *181*, 271-280 e278.

Hoffmann, M., Muller, M.A., Drexler, J.F., Glende, J., Erdt, M., Gutzkow, T., Losemann, C., Binger, T., Deng, H., Schwegmann-Wessels, C.*, et al.* (2013). Differential sensitivity of bat cells to infection by enveloped RNA viruses: coronaviruses, paramyxoviruses, filoviruses, and influenza viruses. PLoS One *8*, e72942.

652 Hoffmann, M., Schroeder, S., Kleine-Weber, H., Muller, M.A., Drosten, C., and Pohlmann, S.

653 (2020c). Nafamostat Mesylate Blocks Activation of SARS-CoV-2: New Treatment Option for

654 COVID-19. Antimicrob Agents Chemother *64*.

655 Kleine-Weber, H., Elzayat, M.T., Hoffmann, M., and Pohlmann, S. (2018). Functional analysis of

656 potential cleavage sites in the MERS-coronavirus spike protein. Sci Rep *8*, 16597.

657 Kleine-Weber, H., Elzayat, M.T., Wang, L., Graham, B.S., Muller, M.A., Drosten, C., Pohlmann,

658 S., and Hoffmann, M. (2019). Mutations in the Spike Protein of Middle East Respiratory

659 Syndrome Coronavirus Transmitted in Korea Increase Resistance to Antibody-Mediated

660 Neutralization. J Virol *93*.

661 Korber, B., Fischer, W.M., Gnanakaran, S., Yoon, H., Theiler, J., Abfalterer, W., Hengartner, N.,

662 Giorgi, E.E., Bhattacharya, T., Foley, B.*, et al.* (2020). Tracking Changes in SARS-CoV-2 Spike:

663 Evidence that D614G Increases Infectivity of the COVID-19 Virus. Cell *182*, 812-827 e819.

664 Leung, K., Shum, M.H., Leung, G.M., Lam, T.T., and Wu, J.T. (2021). Early transmissibility

665 assessment of the N501Y mutant strains of SARS-CoV-2 in the United Kingdom, October to

666 November 2020. Euro Surveill *26*.

667 Monteil, V., Kwon, H., Prado, P., Hagelkruys, A., Wimmer, R.A., Stahl, M., Leopoldi, A.,

668 Garreta, E., Hurtado Del Pozo, C., Prosper, F.*, et al.* (2020). Inhibition of SARS-CoV-2

669 Infections in Engineered Human Tissues Using Clinical-Grade Soluble Human ACE2. Cell *181*,

670 905-913 e907.

671 Muik, A., Wallisch, A.K., Sanger, B., Swanson, K.A., Muhl, J., Chen, W., Cai, H., Maurus, D.,

672 Sarkar, R., Tureci, O.*, et al.* (2021). Neutralization of SARS-CoV-2 lineage B.1.1.7 pseudovirus

673 by BNT162b2 vaccine-elicited human sera. Science.

674 Peng, Y., Mentzer, A.J., Liu, G., Yao, X., Yin, Z., Dong, D., Dejnirattisai, W., Rostron, T.,

675 Supasa, P., Liu, C.*, et al.* (2020). Broad and strong memory CD4(+) and CD8(+) T cells induced

676 by SARS-CoV-2 in UK convalescent individuals following COVID-19. Nat Immunol *21*, 1336-

677 1345.

678   Plante, J.A., Liu, Y., Liu, J., Xia, H., Johnson, B.A., Lokugamage, K.G., Zhang, X., Muruato,

679   A.E., Zou, J., Fontes-Garfias, C.R*., et al.* (2020). Spike mutation D614G alters SARS-CoV-2

680   fitness. Nature.

681   Polack, F.P., Thomas, S.J., Kitchin, N., Absalon, J., Gurtman, A., Lockhart, S., Perez, J.L., Perez

682   Marc, G., Moreira, E.D., Zerbini, C*., et al.* (2020). Safety and Efficacy of the BNT162b2 mRNA

683   Covid-19 Vaccine. N Engl J Med.

684   Rodda, L.B., Netland, J., Shehata, L., Pruner, K.B., Morawski, P.A., Thouvenel, C.D., Takehara,

685   K.K., Eggenberger, J., Hemann, E.A., Waterman, H.R*., et al.* (2020). Functional SARS-CoV-2-

686   Specific Immune Memory Persists after Mild COVID-19. Cell.

687   Sauer, A.K., Liang, C.H., Stech, J., Peeters, B., Quere, P., Schwegmann-Wessels, C., Wu, C.Y.,

688   Wong, C.H., and Herrler, G. (2014). Characterization of the sialic acid binding activity of

689   influenza A viruses using soluble variants of the H7 and H9 hemagglutinins. PLoS One *9*,

690   e89529.

691   Volz, E., Hill, V., McCrone, J.T., Price, A., Jorgensen, D., O'Toole, A., Southgate, J., Johnson,

692   R., Jackson, B., Nascimento, F.F*., et al.* (2021). Evaluating the Effects of SARS-CoV-2 Spike

693   Mutation D614G on Transmissibility and Pathogenicity. Cell *184*, 64-75 e11.

694   Wajnberg, A., Amanat, F., Firpo, A., Altman, D.R., Bailey, M.J., Mansour, M., McMahon, M.,

695   Meade, P., Mendu, D.R., Muellers, K*., et al.* (2020). Robust neutralizing antibodies to SARS-

696   CoV-2 infection persist for months. Science *370*, 1227-1230.

697   Wang, Y., Zhang, D., Du, G., Du, R., Zhao, J., Jin, Y., Fu, S., Gao, L., Cheng, Z., Lu, Q*., et al.*

698   (2020). Remdesivir in adults with severe COVID-19: a randomised, double-blind, placebo-

699   controlled, multicentre trial. Lancet *395*, 1569-1578.

700   Weissman, D., Alameh, M.G., de Silva, T., Collini, P., Hornsby, H., Brown, R., LaBranche, C.C.,

701   Edwards, R.J., Sutherland, L., Santra, S*., et al.* (2021). D614G Spike Mutation Increases SARS

702   CoV-2 Susceptibility to Neutralization. Cell Host Microbe *29*, 23-31 e24.

703   Xia, S., Liu, M., Wang, C., Xu, W., Lan, Q., Feng, S., Qi, F., Bao, L., Du, L., Liu, S*., et al.*

704   (2020). Inhibition of SARS-CoV-2 (previously 2019-nCoV) infection by a highly potent pan-

705   coronavirus fusion inhibitor targeting its spike protein that harbors a high capacity to mediate

706   membrane fusion. Cell Res *30*, 343-355.

707   Xie, X., Liu, Y., Liu, J., Zhang, X., Zou, J., Fontes-Garfias, C.R., Xia, H., Swanson, K.A., Cutler,

708   M., Cooper, D*., et al.* (2021). Neutralization of SARS-CoV-2 spike 69/70 deletion, E484K and

709   N501Y variants by BNT162b2 vaccine-elicited sera. Nat Med.

710   Zhao, S., Lou, J., Cao, L., Zheng, H., Chong, M.K.C., Chen, Z., Chan, R.W.Y., Zee, B.C.Y.,

711   Chan, P.K.S., and Wang, M.H. (2021). Quantifying the transmission advantage associated with

712   N501Y substitution of SARS-CoV-2 in the United Kingdom: An early data-driven analysis. J

713   Travel Med.

714   Zhou, P., Yang, X.L., Wang, X.G., Hu, B., Zhang, L., Zhang, W., Si, H.R., Zhu, Y., Li, B.,

715   Huang, C.L*., et al.* (2020). A pneumonia outbreak associated with a new coronavirus of probable

716   bat origin. Nature *579*, 270-273.

717

718

719

720

721

722

723

724

725

726

727

728

729

730 **FIGURE LEGENDS**

731

732 **Figure 1. Schematic overview of the S proteins from the SARS-CoV-2 variants under study**

733 The location of the mutations in the context of spike protein domain organization is shown in the

734 upper panel. RBD = receptor binding domain, TD = transmembrane domain. The location of the

735 mutations in the context of the trimer spike protein domain is shown lower panel. Color code:

736 light blue = S1 subunit with RBD in dark blue, grey = S2 subunit, orange = S1/S2 and S2'

737 cleavage sites, red = mutated amino acid residues.

738

739 **Figure 2. S proteins from SARS-CoV-2 variants drive entry into human cell lines**

740 (A) Directed expression of SARS-CoV-2 S proteins (SARS-2-S) in A549-ACE2 cells leads to the

741 formation of syncytia. S protein expression was detected by immunostaining using an antibody

742 directed against a C-terminal HA-epitope tag. Presented are the data from one representative

743 experiment. Similar results were obtained in four biological replicates.

744 (B) The S proteins of the SARS-CoV-2 variants mediate robust entry into cell lines. The

745 indicated cell lines were inoculated with pseudotyped particles bearing the S proteins of the

746 indicated SARS-CoV-2 variants. Transduction efficiency was quantified by measuring virus-

747 encoded luciferase activity in cell lysates at 16-20 h post transduction. Presented are the average

748 (mean) data from six biological replicates (each conducted with technical quadruplicates). Error

749 bars indicate the standard error of the mean (SEM). Statistical significance was analyzed by one-

750 way analysis of variance (ANOVA) with Dunnett's posttest. WT = wildtype, GB = Great Britain,

751 SA = South Africa, BRA = Brazil

752

31

753 **Figure 3. The S proteins of the SARS-CoV-2 variants drive robust cell-cell fusion**

754 (A) Quantitative cell-cell fusion assay. S protein-expressing effector cells were mixed with ACE2

755 or ACE2/TMPRSS2 expressing target cells and cell-cell fusion was analyzed by measuring

756 luciferase activity in cell lysates. Presented are the average (mean) data from four biological

757 replicates. Error bars indicate the SEM. Statistical significance was analyzed by one-way

758 ANOVA with Dunnett's posttest.

759 (B) Qualitative fusion assay. A549-ACE2 (left) and A549-ACE2/TMPRSS2 (right) cells were

760 transfected to express the indicated S proteins (or no viral protein) along with DsRed. At 24 h

761 posttransfection, cells were fixed and analyzed for the presence of syncytia by fluorescence

762 microscopy (magnification: 10x). Presented are representative images from a single experiment.

763 Data were confirmed in three additional experiments. WT = wildtype, GB = Great Britain, SA =

764 South Africa, BRA = Brazil

765

766 **Figure 4. Particles bearing the S proteins of SARS-CoV-2 variants exhibit similar stability**

767 **and entry kinetics**

768 (A) Particles bearing the indicated S proteins were incubated for different time intervals at 33 °C,

769 snap frozen, thawed and inoculated onto Vero cells. Entry of particles that were frozen

770 immediately was set as 100%.

771 (B) Particles bearing the indicated S proteins were incubated for indicated time intervals with

772 Vero cells. Subsequently, the cells were washed and luciferase activity determined. Transduction

773 measured without particle removal by washing was set as 100%.

774 For both panels, the average (mean) data from three biological replicates (each performed with

775 technical quadruplicates) is presented. Error bars indicate the SEM. Statistical significance was

776   analyzed by one-way ANOVA with Dunnett's posttest. WT = wildtype, GB = Great Britain, SA

777   = South Africa, BRA = Brazil

778

779   **Figure 5. Entry driven by the S proteins of the SARS-CoV-2 variants can be blocked with**

780   **soluble ACE2, protease inhibitors targeting TMPRSS2 and a membrane fusion inhibitor**

781   Top row, left panel: S protein-bearing particles were incubated with different concentrations of

782   soluble ACE2 (30 min, 37 °C) before being inoculated onto Vero cells. Top row, middle and

783   right panel: Caco-2 target cells were pre-incubated with different concentrations of serine

784   protease inhibitors (Camostat or Nafamostat; 1 h, 37 °C) before being inoculated with particles

785   harboring the indicated S proteins. Bottom row, both panels: The peptidic fusion inhibitor EK-1

786   and its improved lipidated derivate EK-1-C4 were incubated with partices at indicated

787   concentrations (30 min, 37 °C) and then added to Vero cells. All panels: Transduction efficiency

788   was quantified by measuring virus-encoded luciferase activity in cell lysates at 16-20 h

789   posttransduction. For normalization, inhibition of SARS-2-S-driven entry in samples without

790   soluble ACE2 or inhibitor was set as 0 %. Presented are the average (mean) data from three

791   biological replicates (each performed in technical triplicates [EK-1, EK-1-C4] or quadruplicates

792   [soluble ACE2, Camostat, Nafamostat]). Error bars indicate the SEM. Statistical significance was

793   analyzed by one-way ANOVA with Dunnett's posttest. WT = wildtype, GB = Great Britain, SA

794   = South Africa, BRA = Brazil

795

796   **Figure 6. The S proteins of SARS-CoV-2 variants from South Africa and Brazil are**

797   **partially or fully resistant to inhibition by therapeutic monoclonal antibodies with EUA**
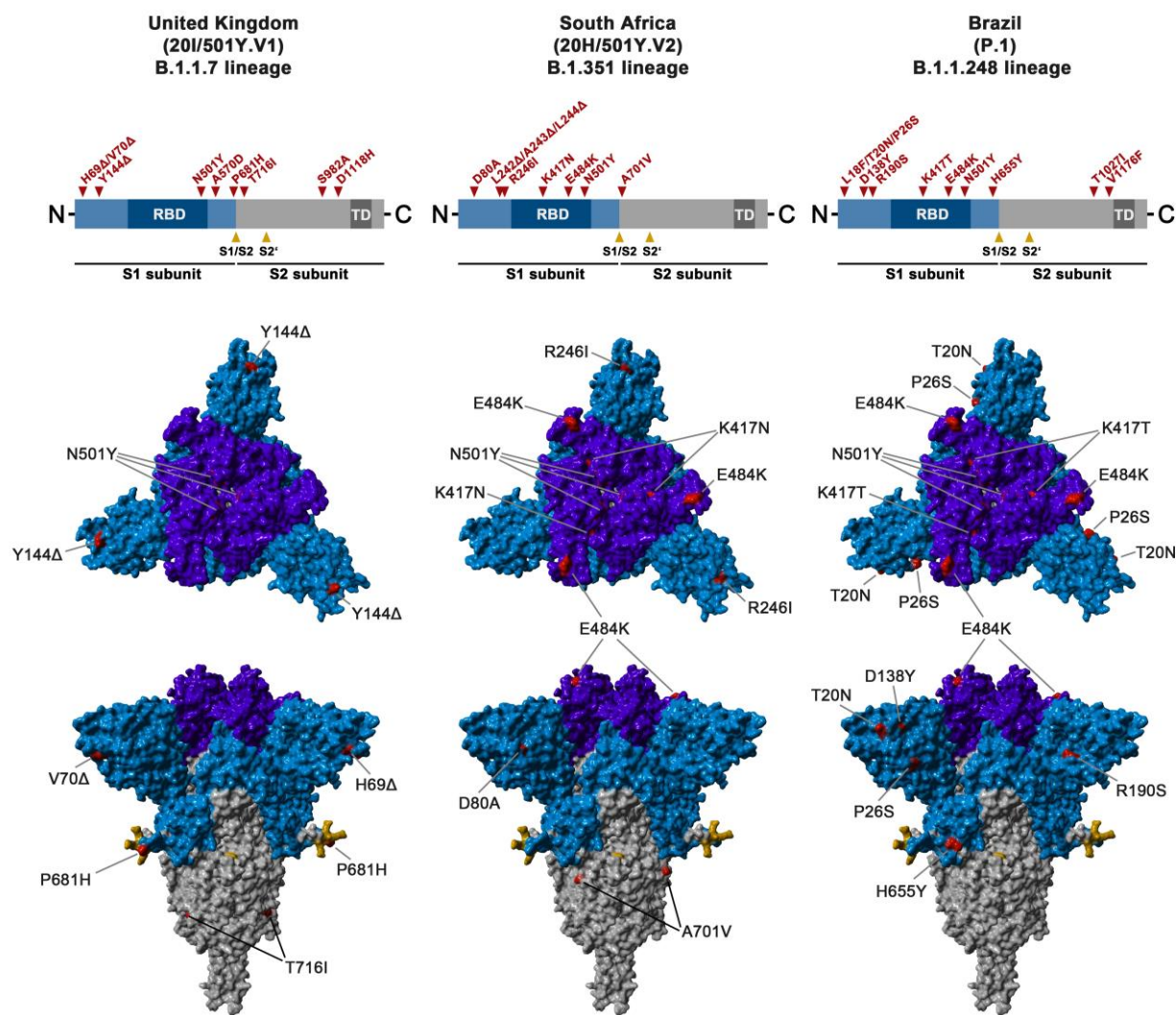
798   Pseudotypes bearing the indicated S proteins were incubated (30 min, 37 °C) with different

799   concentrations of control antibody (hIgG), three different Regeneron antibodies (Casirivimab,

33

800   Imdevimab, REGN10989) or Bamlanivimab (LY-CoV555) before being inoculated onto target

801   Vero cells. Transduction efficiency was quantified by measuring virus-encoded luciferase activity

802   in cell lysates at 16-20 h posttransduction. For normalization, inhibition of S protein-driven entry

803   in samples without antibody was set as 0 %. Presented are the data from a single experiment

804   performed with technical triplicates. Data were confirmed in a separate experiment. Error bars

805   indicate standard deviation (SD). WT = wildtype, GB = Great Britain, SA = South Africa, BRA =

806   Brazil

807

808   **Figure 7. S proteins of SARS-CoV-2 variants from South Africa and Brazil show reduced**

809   **neutralization sensitivity against convalsecent plasma and serum from BNT162b2**

810   **vaccinated individuals**

811   Pseudotypes bearing the indicated S proteins were incubated (30 min, 37 °C) with different

812   dilutions of plasma derived from COVID-19 patients (A) or serum from individuals vaccinated

813   with the Pfizer/BioNTech vaccine BNT162b2 (obtained 13-15 days after the second dose) and

814   inoculated onto Vero target cells. Transduction efficiency was quantified by measuring virus-

815   encoded luciferase activity in cell lysates at 16-20 h posttransduction. The results are shown as %

816   inhibition. For normalization, S protein-driven entry in the absence of plasma/serum was set as 0

817   %. Presented are the data from a single experiment performed with technical triplicates. Error

818   bars indicate SD. Results were confirmed in a second biological replicate. (C) Serum dilutions

819   that lead to a 50% reduction in S protein-driven transduction (neutralization titer 50, NT50) were

820   calculated for convalsecent plasma (left) and vaccinee sera (right). Presented are the data derived

821   from panels A and B. The line indicates the median. WT = wildtype, GB = Great Britain, SA =
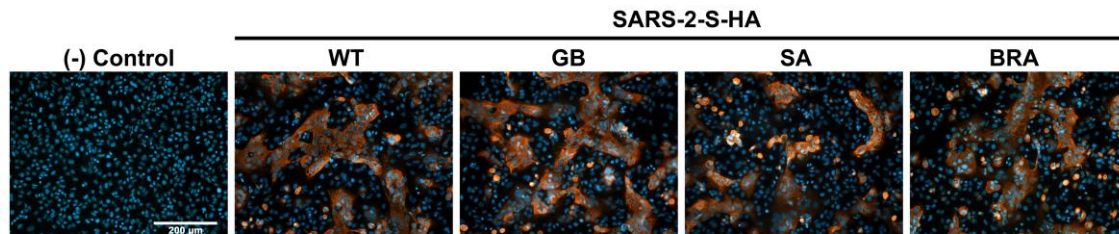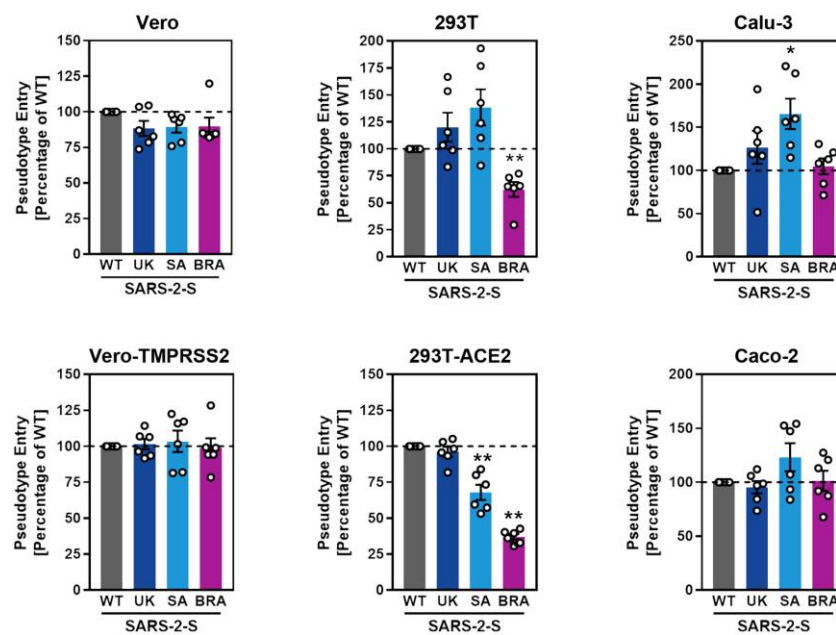
822   South Africa, BRA = Brazil
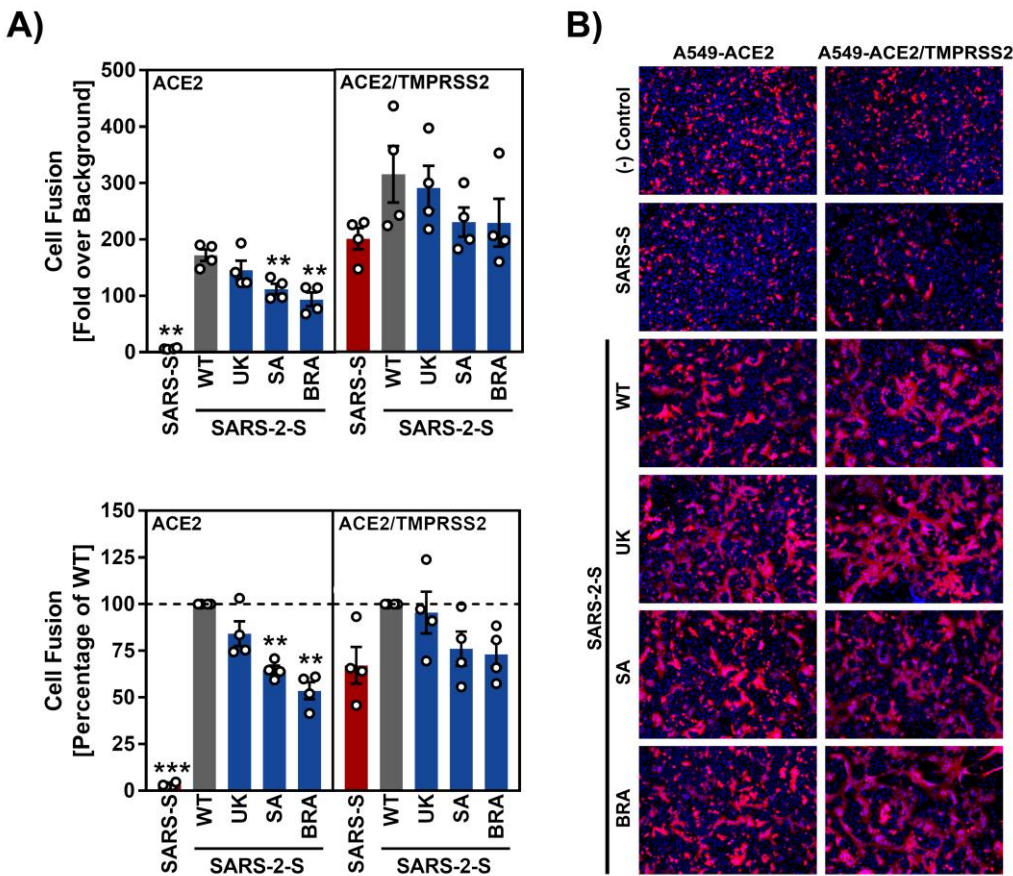
823

34

Figure 1

824

825

Figure 2
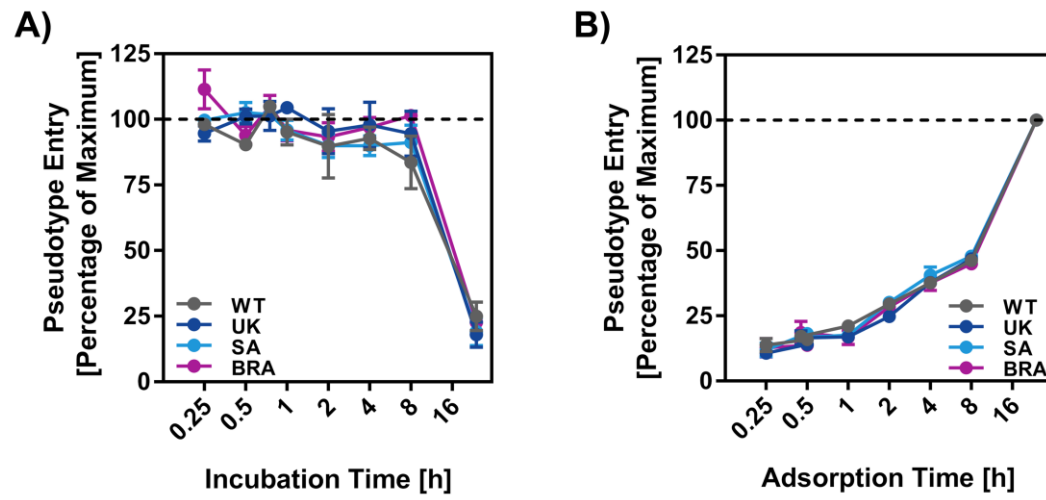
A)

B)

826

827
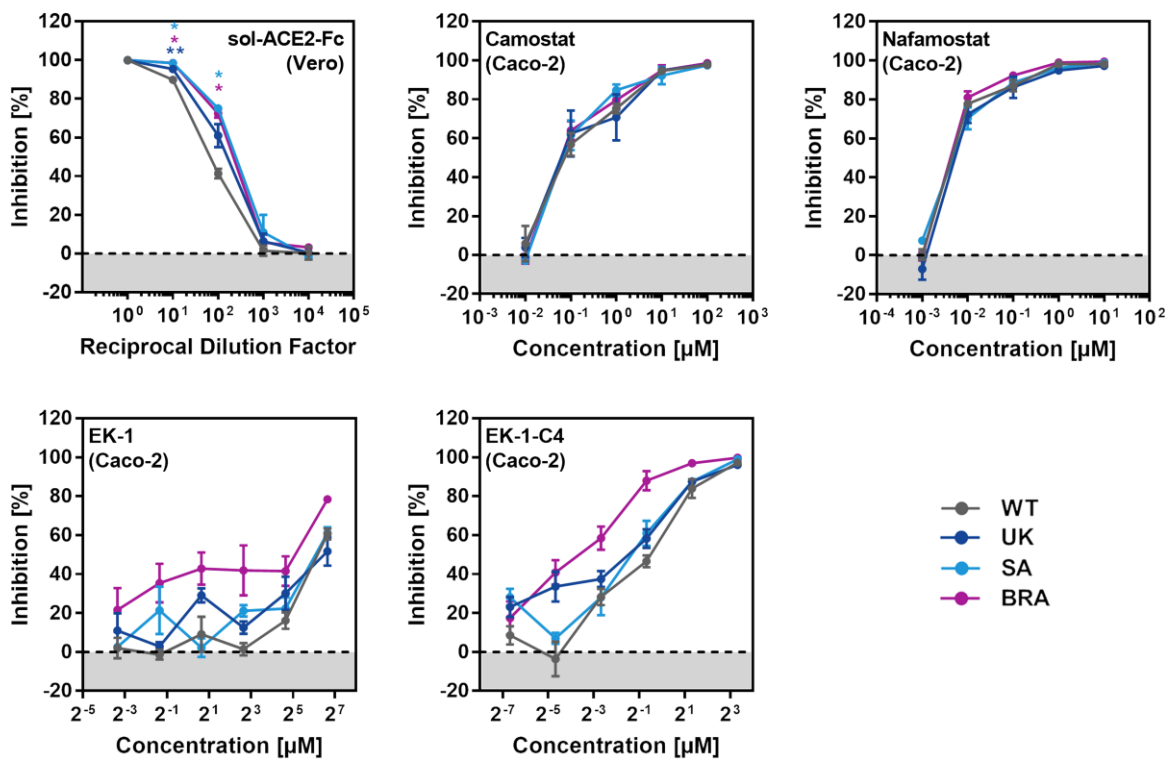
Figure 3

828

829

37
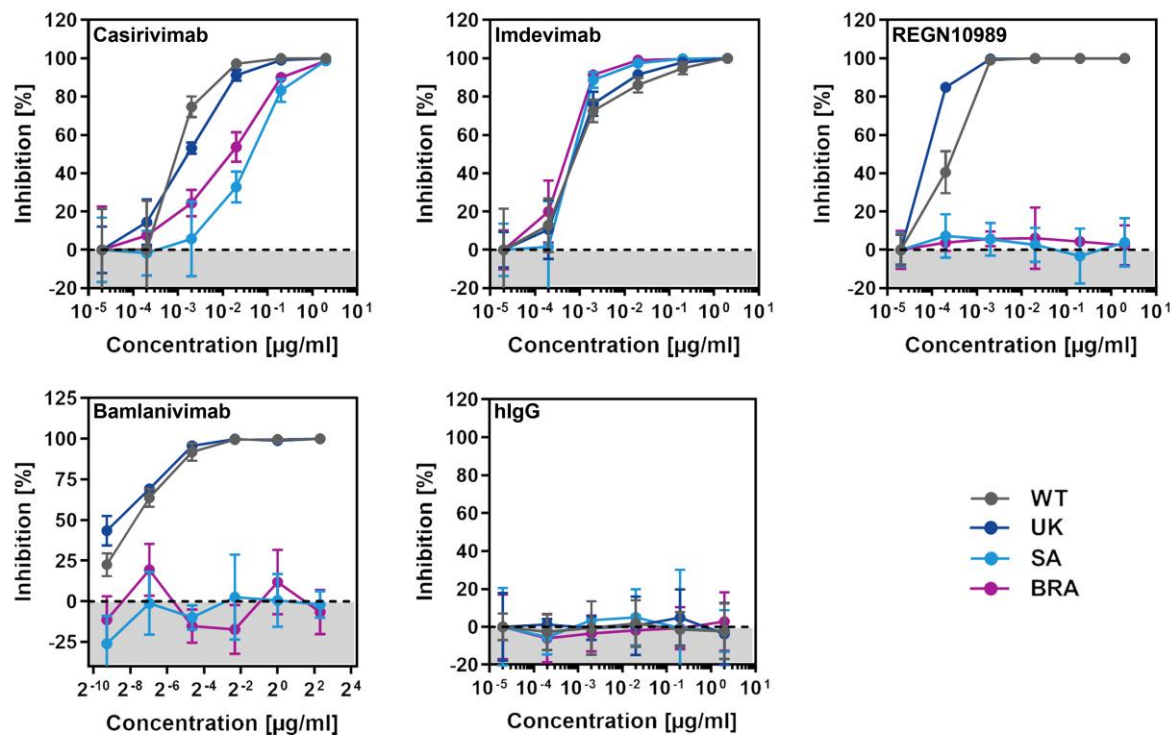
Figure 4

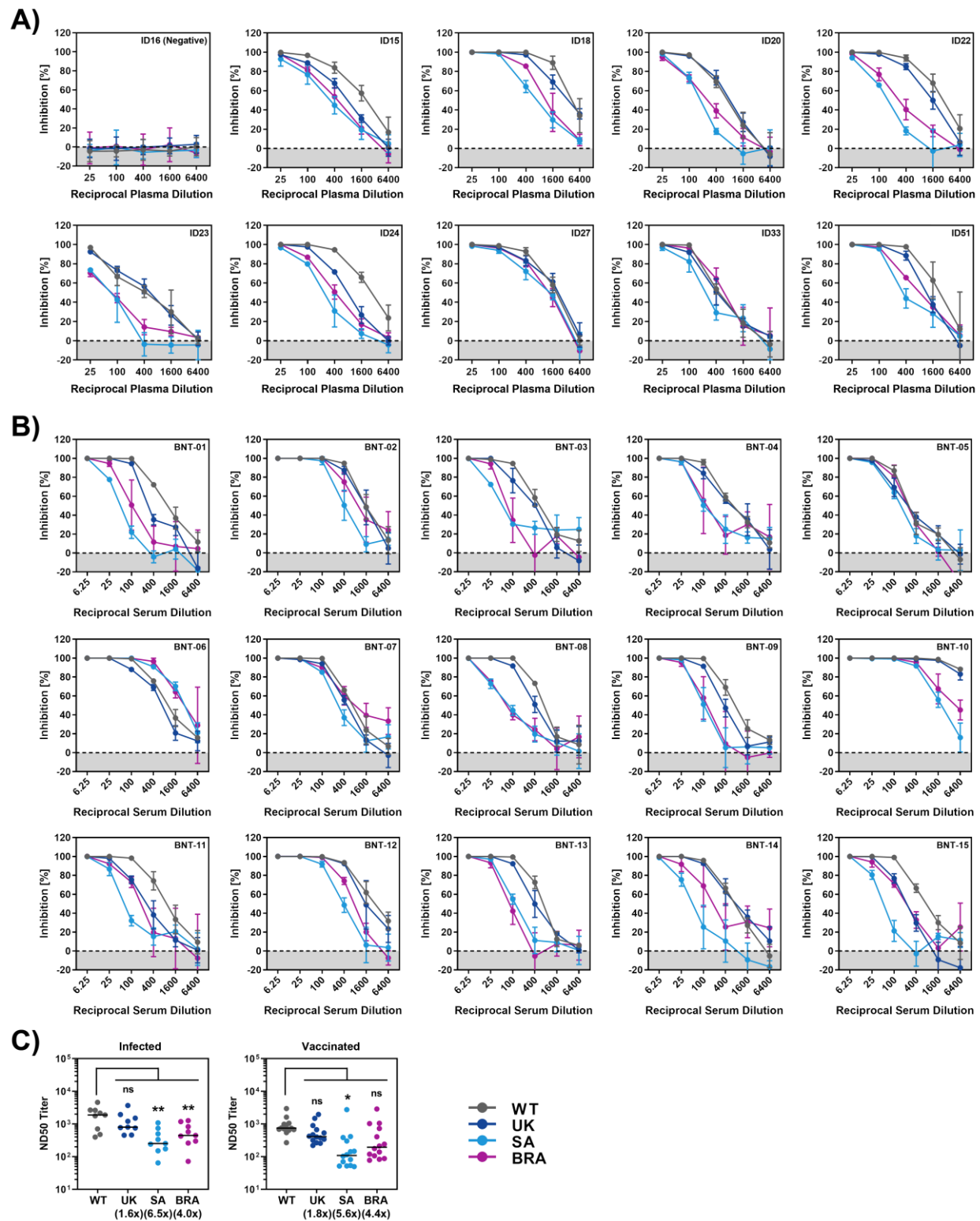830

831

Figure 5

832

833

Figure 6

834

835

Figure 7

838 **Table S1:** BNT162b2-vaccinated patient data. Serological data shows antibody titer against Spike

839 (IgG, IgA) and Nucleocapsid (NCP, IgG) protein measured by Euroimmun-ELISA, values are

840 given as baseline-corrected OD ratios compared to a calibrator. For all analytes, a ratio < 0.8 was

841 considered to be non-reactive or negative. An OD-ratio of ≥ 1.1 was considered to be positive for

842 all three analytes.

843

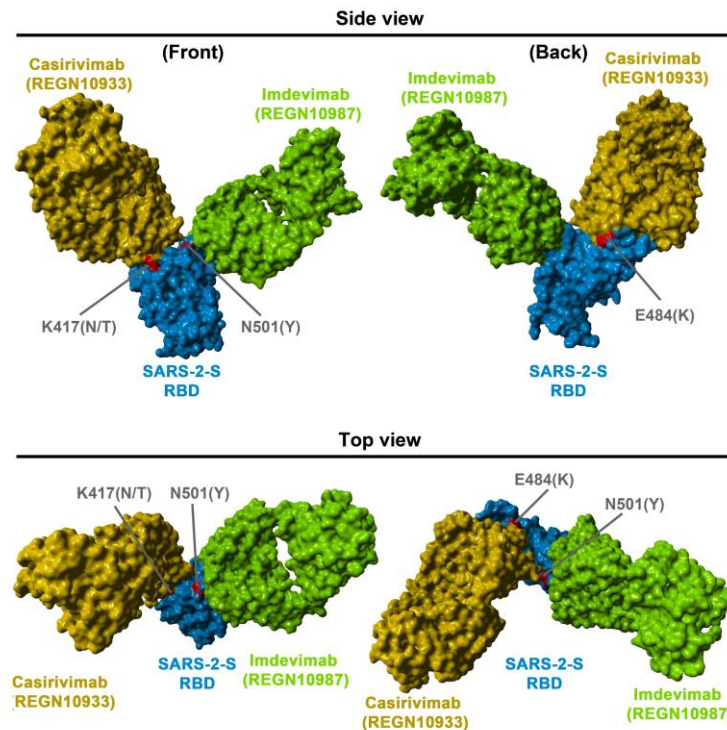| ID	Age (y)	Gender	Time since 2nd vaccination (d)	Spike-IgG	Spike-IgA	NCP-IgG
BNT-1	32	f	14	8.72	>9	0.06
BNT-2	25	f	14	>9	>9	0.06
BNT-3	41	m	13	8.46	>9	0.06
BNT-4	48	m	14	>9	>9	0.07
BNT-5	51	m	14	8.53	6.61	0.08
BNT-6	38	m	14	8.76	8.07	0.04
BNT-7	45	f	14	>9	>9	0.08
BNT-8	55	f	14	>9	8.47	0.03
BNT-9	38	m	15	>9	>9	0.19
BNT-10	41	m	14	>9	>9	0.06
BNT-11	44	f	14	>9	>9	0.06
BNT-12	41	m	14	>9	8.12	0.07
BNT-13	43	m	14	>9	5.3	0.05
BNT-14	65	m	13	>9	>9	0.39
BNT-15	32	m	15	>9	>9	0.03

844

SI Figure S1

A)

845

846 **Fígure S1.** Location of SARS-2-S RBD mutations K417N/T, E484K and N501Y with respect to

847 the binding interface of the REGN-COV2 antibody cocktail (related to Figure 6).

848 The protein models of the SARS-2-S receptor-binding domain (RBD, blue) in complex with

849 antibodies Casirivimab (REGN10933, orange) and Imdevimab (REGN10987, green) were

850 constructed based on the 6XDG template (Hansen et al., 2020). Residues highlighted in red

851 indicate amino acid variations found in emerging SARS-CoV-2 variants from the United

852 Kingdom, South Africa and Brazil.

853